Computer Methods and Programs in Biomedicine 240 (2023) 107701

Contents lists available at ScienceDirect

Computer Methods and Programs in Biomedicine

journal homepage: www.elsevier.com/locate/cmpb

Comparative study of neonatal brain injury fetuses using machine learning methods for perinatal data

Qingjun Cao[a], Hongzan Sun[b], Hua Wang[a], Xueyan Liu[a], Yu Lu[c], Liang Huo[a,*]

[a] Department of Pediatrics, Shengjing Hospital of China Medical University, Shenyang 110004, China
[b] Department of Radiology, Shengjing Hospital of China Medical University, Shenyang 110004, China
[c] College of Big Data and Internet, Shenzhen Technology University, Shenzhen 518118, China

ARTICLE INFO

Article history:
Received 4 May 2021
Revised 20 June 2023
Accepted 28 June 2023

Keywords:
Machine learning
Perinatal period
Suffocation
Brain damage
Hemodynamics

ABSTRACT

Objective: CTG is used to record the fetus's fetal heart rate and uterine contraction signal during pregnancy. The prenatal fetal intrauterine monitoring level can be used to evaluate the fetal intrauterine safety status and reduce the morbidity and mortality of the perinatal fetus. Perinatal asphyxia is the leading cause of neonatal hypoxic-ischemic encephalopathy and one of the leading causes of neonatal death and disability. Severe asphyxia can cause brain and permanent nervous system damage and leave different degrees of nervous system sequelae.

Methods: This paper evaluates the classification performance of several machine learning methods on CTG and provides the auxiliary ability of clinical judgment of doctors. This paper uses the data set on the public database UCI, with 2126 samples.

Results: The accuracy of each model exceeds 80%, of which XGBoost has the highest accuracy of 91%. Other models are Random tree (90%), light (90%), Decision tree (83%), and KNN (81%). The performance of the model in other indicators is XGBoost (precision: 90%, recall: 93%, F1 score: 90%), Random tree (precision: 88%, recall: 91%, F1 score: 89%), lightGBM (precision: 87%, recall: 93%, F1 score: 90%), Decision tree (precision: 83%, recall: 86%, F1 score: 84%), KNN (precision: 77%, recall: 85%, F1 score: 81%).

Conclusion: The performance of XGBoost is the best of all models. This result also shows that using the machine learning method to evaluate the fetus's health status in CTG data is feasible. This will also provide and assist doctors with an objective assessment to assist in clinical diagnosis.

1. Introduction

In 2021, academician Qiao Jie of the Third Hospital of Peking University, Director Song Li of the Maternal and Child Department of the National Health Commission of China, and Professor Zhu Jun of the national maternal and child health monitoring office of Sichuan University were co correspondents, and 31 experts and scholars from well-known institutions at home and abroad were co-authors. They published a report in the Lancet [1]. The report pointed out that since 1949, China has made remarkable achievements in improving maternal and infant survival. The neonatal mortality rate decreased every year. In 2015, the gap between the average neonatal mortality rate in North America and Europe narrowed to 1.7 times. However, due to China's large population base, neonatal deaths will be higher. According to "Born Too Soon: The Global Action Report on Preterm Birth" released by World Health Organization (WHO), among about 15 million preterm infants, the number of preterm infants in China ranks second in the world. Maternal and newborn health is an integral part of maternal and child health. Its main challenges include maternal safety (reducing postpartum hemorrhage and indirect obstetric causes of death), stillbirth, premature birth, congenital disabilities, etc.

The objective of using CTG (Cardiotocography) during pregnancy is to record the fetal heart rate and uterine contraction signal of the fetus. It helps in evaluating the fetal intrauterine safety status and reducing the morbidity and mortality of the perinatal fetus. The health status of the fetus is directly related to the perinatal health status of the newborn. Perinatal asphyxia is the leading cause of neonatal hypoxic-ischemic encephalopathy and one of the leading causes of neonatal death and disability. Perinatal asphyxia refers to a condition where the newborn experiences a lack of oxygen before, during, or immediately after birth. It is the main cause of neonatal hypoxic-ischemic encephalopathy and can lead to brain damage, permanent nervous system damage, and different degrees of nervous system sequelae. Evaluating the classification performance of several machine learning methods on CTG can pro-

* Corresponding author.
E-mail address: huol@sj-hospital.org (L. Huo).

https://doi.org/10.1016/j.cmpb.2023.107701
0169-2607/

vide the auxiliary ability for doctors to make the correct diagnosis and treatment. The purpose of the mentioned research paper is to evaluate the classification performance of various machine learning methods on CTG data. It aims to provide an auxiliary ability for clinical doctors to make judgments based on the analysis of CTG data.

2. Methods and datasets

2.1. Data materials

The research paper used a dataset from the public database UCI, consisting of a total of 2126 samples. One hundred twenty asphyxiated premature infants born in the obstetrics department of our hospital from January 2015 to December 2022 were selected as the research subjects. Inclusion criteria: ① gestational age<37 weeks; ② meets the diagnostic criteria for neonatal asphyxia [2], with an Apgar score of<8 points at 1 min after birth. Premature infants exhibit cyanosis, bradycardia, hypotension, respiratory depression, and hypotonia; ③ Single birth, with a premature mother under 35 years old, is regularly examined and delivered at our hospital. Exclusion criteria: deformed infants, congenital heart disease, infections, and transferred premature infants. According to the 1-minute Apgar score after birth, there were 71 cases in the mild asphyxia group (4–7 points in the 1-minute Apgar score) and 51 cases in the severe asphyxia group ($\leq$ 3 points in the 1-minute Apgar score and still $\leq$ 5 points in the 5-minute Apgar score). At the same time, 45 healthy premature infants with no history of asphyxia and an Apgar score of 8–10 at 1 min after birth were selected and included in the control group. The hospital ethics committee approved this study, and the parents of premature infants signed an informed consent form.

2.2. Magnetic resonance imaging (MRI) protocol

The MRI machine is Philips Intera Achieva 3.0t superconducting magnetic resonance imaging equipment. Conventional MRI scanning included T1-weighted imaging (T1WI), T2-weighted imaging (T2WI), Flair, and DWI. The parameters included: T1WI: repetition time (TR)= 1920 ms, echo time (TE)=2.5 ms, field of view (FOV)=260 mm, slices=178, slice thickness=1.0 mm, and bandwidth=160. T2WI: TR=3240 ms, TE=88 ms, FOV=260 mm, slices=30, slice thickness=3.0 mm. DTI: TR=5580 ms, TE=94 ms, FOV=260 mm. Two times for collection.

2.3. Dataset usage

The dataset used in this article is open-source data from UCI [3]. The dataset is CTG data with indicative characteristics obtained from the CTG automatic analysis system [4]. There are 2126 CTs in this dataset. Three obstetric experts evaluated the CTG data.

Table 1
Data feature attribute information table.

For Short	Detailed Name
LB	FHR Baseline (heartbeats per 60 s)
AC	Acceleration per second
FM	Fetal Movements Per Second
UC	Uterine contractions per second
DL	Monitored amount of light deceleration per second
DS	Number of monitors for severe slowdowns per second
DP	Number of monitors per second for long deceleration
ASTV	Percentage of time monitoring data is abnormal in short-term variation
MSTV	Surveillance data in short-term variation mean
ALTV	Percentage of Long-Term Monitored Variant Abnormalities
MLTV	Mean of long-term monitoring variation data
Width	Width of the FHR histogram raw data plot
Min	Minimum value for FHR histogram raw data plot
Max	Maximum value of FHR histogram raw data plot
Nmax	Number of peaks in the histogram raw measurement data
Nzeros	Number of zero points in the histogram of raw data
Mode	Raw data histogram mode
Mean	Raw data histogram mean value
Median	The median value in the raw data histogram
Variance	Raw data histogram variance value
Trend	Raw data histogram trend values
CLASS	FHR Surveillance Data Mode Class Code (1 to 10)
NSP	Monitoring data fetal status category code (*N*=normal value; *S*=suspicious value; *P*=pathological value)

Table 1: The features provided in the dataset and their explanations. The dataset provides 23 features, with categories being morphological patterns and NSP being fetal status. Therefore, the database can use two types of experiments. The label used in this article is NSP, which is divided into three categories (N is normal, S is suspicious, and P is pathological). This article uses NSP as the label for the experiment. This section will introduce the learning methods used in the experiment as follows:

2.4. KNN

The Neighborhood Algorithm (KNN) [5] is a simple and commonly used machine learning algorithm. The principle is simple: when predicting sample x, find the category with the highest proportion based on the first k samples closest to it, and then the predicted sample x is its category. The distance between samples is usually calculated by Euclidean distance, and its formula is as follows:

$$d_E = \sum_{i=1}^{N} \sqrt{x_i^2 + y_i^2}$$

x_i is the value under the dimension. After calculating the distance between sample x and all points in the plane, sort and select the first k samples with the shortest distance to predict x. The value of k will affect the prediction results, as shown in Fig. 1.

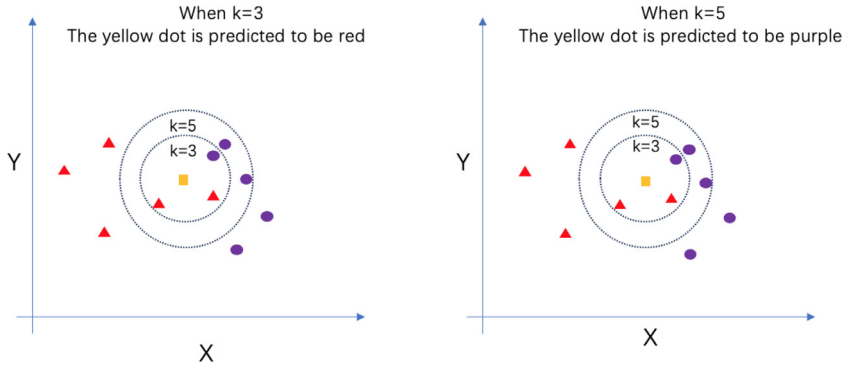

Fig. 1. Samples under different K values *x*.

Cross-validation is possible. Firstly, select a smaller K value, calculate the variance in the validation set, and gradually increase to find the appropriate K value.

2.5. Decision tree

A decision tree [6] is a simple method with a reliable explanatory power that aligns with human intuitive thinking. Decision trees classify data through a series of rules. The decision tree consists of decision nodes, branches, and leaf nodes. Each non-leaf node serves as a decision node, determines the incoming branch through certain conditions, and ultimately reaches the leaf node. Leaf nodes represent the results of the sample. The role of decision nodes is to use data characteristics to partition data, making unordered data orderly. Some quantitative criteria determine the selection of features—the classification and regression tree (Cart) used in this article [7].

When Cart predicts discrete data. The Gini index selects the optimal feature and determines the optimal binary segmentation point. Assuming the dataset has *K* categories and the probability of the sample belonging to *K* categories is *Pk*, the Gini index of the sample is defined as:

$$Gini(p) = \sum_{k=1}^{m} Pk\left(1 - Pk\right) = 1 - \sum_{k=1}^{K} p_k^2$$

According to the definition of the Gini index, the Gini index of dataset *D* can be obtained, where *CK* represents a subset of dataset *D* that belongs to the *K* class.

$$Gini(D) = 1 - \sum_{k=1}^{K} \left(\frac{|C_k|}{D}\right) x^2$$

If dataset *D* is divided based on *a* particular value of feature a to obtain two subsets, D_1 and D_2, the Gini coefficients under feature a are as follows: *Gini* (*D*) represents the uncertainty in set *D*, and the following equation represents the uncertainty after dividing feature *a* by $a = a$. The larger the value, the greater the uncertainty of the set:

$$Gain\_Gini(D, A) = \frac{|D1|}{|D|} Gini(D_1) + \frac{|D1|}{|D|} Gini(D_2)$$

For feature A, it is possible to calculate the *Gain_Gini* and choose the smallest value as the segmentation value of feature A, which can serve as the decision node of the decision tree.

2.6. Integrated learning

Ensemble learning is achieved by constructing multiple weak classifiers to complete the learning task, as shown in Fig. 2. Multiple weak learners are trained in different ways and combined through some strategies to form a classification system. Boosting [8–9] and Bagging [10] are ensemble learning methods. Bagging's classifiers are interdependent and require continuous training. Bagging will train a primary classifier from the initial dataset, and subsequent classifiers need to pay more attention to the samples misclassified by the previous classifier, continue in sequence, directly generate a specified number of classifiers, and finally combine them in a weighted manner. Boosting is a parallel method. There is no strong dependency between classifiers, so that parallel training can be carried out. Bagging is: given a dataset D, select one at a time. After selection, return the samples to dataset D so that they can still be selected next time. By selecting N times, obtain a sub-dataset of N samples (which may contain duplicate samples), and then train the dataset as a classifier. According to this method, K classifiers are obtained by repeating and combining K times. The classification strategy is usually the voting method, as shown in Fig. 2:

2.6.1. random forest model

Random forest [11] belongs to the Bagging method in set learning. The random forest comprises multiple decision trees, and there is no correlation between different decision trees. When forecasting and classifying the samples, the decision tree of each category in the random forest is used for forecasting and classification, and the one with the most classification results is selected as the final prediction result of the samples.

The rule of decision tree generation in the random forest is: to select one in dataset D at a time, put it back into dataset D after selection, and select N samples to form the training set of the decision tree. Randomly select a subset of X features from all the features in the sub-dataset, select a strategy to generate a decision tree, and train the decision tree. Thus generating multiple different decision trees.

2.6.2. XGBoost

The XGBoost algorithm is an improved Boosting-based algorithm with high predictive power. Its advantage is that L2 regularization is added to the objective function to limit the tree's growth and the splitting of nodes and to prevent the value of nodes from being too high (too high values tend to lead to overfitting). The core algorithm of XGBoost is:

We are continuously adding decision trees and splitting features to generate decision trees. Each time a decision tree is added, it learns a new function to fit the residual predicted last time.

$$\hat{y}\_i = \sum\_(t = 1)\^k \; [\![f\_t\,(x\_i\,)]\!]$$

$$F = \{f(x) = w\_q(x)\;\}(q: R\^m \to T, w \in R\^T\,)$$

Where $w\_q(x)$ is the score of leaf node *q*, f corresponds to the set of all *k* trees, and *f*(*x*) is one of them.

2) When we get *k* trees after training, we need to predict the score of a sample. In fact, according to the feature of this sample, each tree will fall to a corresponding leaf node, and each leaf node corresponds to a score.

3) Finally, we add up the corresponding scores of each tree to be the predicted value of the sample.

The goal is to make the predicted value of the tree group $\hat{y}\_i$ as close as possible to the true value *y_i*. Moreover, it can be generalization as much as possible. Therefore, the objective function of XGBoost is as follows:

$$\begin{aligned} L(\phi) &= \Sigma\_i \quad l(y\_i, \hat{y}\_i) + \Sigma\_k \quad \Omega(f\_t) \\ \Omega(f\_t) &= \gamma T + 1/2\;\lambda \|w\_q\|\^2 \\ &= \gamma T + 1/2\;\lambda \Sigma\_(j = 1)\^T \quad w\_j\^2 \end{aligned}$$

The objective function is divided into a loss function and a regularization term. The loss function reveals the training error (the difference between the predicted and actual scores), and the regularization defines the complexity. Where *l* is a differentiable convex loss function, which measures the difference between the predicted and target values. The second term is the complexity of the penalty model (the sum of the complexity of all regression trees). This term contains two parts, one is the total number of leaf nodes, and the other is the L2 regularization term obtained by leaf nodes. This additional regularization term can smooth the learning weight of each leaf node to avoid overfitting.

2.6.3. Lightweight GBM

LightGBM [12] is also a boosting method, compared with XGBoost. XGBoost adopts a hierarchical tree growth strategy, although

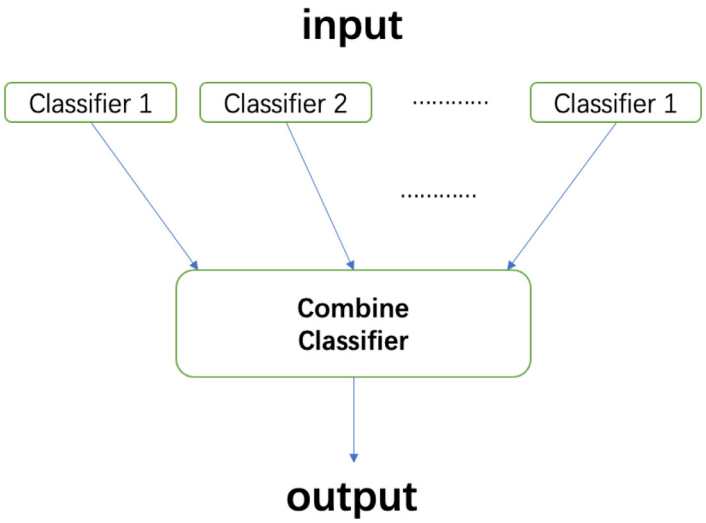

Fig. 2. Co-learning.

it can be optimized in parallel and is not prone to overfitting. However, many nodes have low splitting gain, so searching and splitting them is unnecessary. LightGBM adopts a leaf-by-leaf growth strategy to avoid this issue. Secondly, lightGBM adopts a histogram algorithm, which can significantly reduce the code's running time.

3. Results

This article used five types of machine learning to evaluate CTG data for statistical analysis. The measured data conform to a normal distribution, expressed as mean ± standard deviation ($x \pm s$). Analysis of variance was used for comparison between multiple groups, while the LSD-t-test was used for comparison between two groups. Count data comparison using χ 2 Inspection.

Asphyxiated premature infants undergo magnetic resonance imaging within seven days after birth to observethe effect of asphyxia on the nervous system. Heavy: The posterior horn of the bilateral ventricles is enlarged, and the brain's white matter is generally thinner. DWI shows symmetrical diffuse hyperintense changes in the corpus callosum, basal ganglia, and dorsal thalamus. Extensive white matter injury changes, bilateral posterior horn of the ventricles is widened. Light: T2WI signal of white matter under the cortex of bilateral cerebral hemispheres is increased, small patches of short T1 signal focus are seen near the anterior horn of bilateral ventricles, and DWI shows high signal changes.Brain changes of premature infants, focal white matter injury near the anterior horn of bilateral ventricles. (See Fig. 3).

The incidence of brain injury in three groups of premature infants, from high to low, was ranked as severe asphyxia group, mild asphyxia group, and control group, with statistically significant differences (χ 2 = 17.683, P<0.05), as shown in Table 2.

Table 2
Comparison of the incidence of brain injury in three groups of premature infants [cases (%)].

Group	Number of cases	Brain damage	No brain damage
Severe asphyxia group	40	21(52.40)[ab]	19(47.464)
Mild suffocation group	80	17(19.53)[a]	63(80.51)
Control group	60	2(3.34)	58(96.69)

Note: Compared with the control group, aP<0.05; with the mild asphyxia group, bP<0.05.

The dataset is divided into a training set and a testing set. Each model is fitted with the most suitable parameters for the training set, and the performance of each model is displayed through various evaluation indicators. The results of this model can be divided into four types: true negative (TN), false negative (FN), true positive (TP), and false positive (FP).

Among them, accuracy is the most commonly used method to evaluate the overall performance of a model, referring to predicting the proportion of correct samples among all samples. The formula is as follows:

$$\text{Accuracy} = (\text{TP} + \text{TN})/(\text{TP} + \text{FP} + \text{TN} + \text{FN})$$

Accuracy refers to the proportion of truly positive samples among all predicted positive samples. The formula is as follows:

$$Precision = TP/(TP + FP)$$

Recall refers to the correct proportion of all positive samples predicted by the model. The formula is as follows:

$$Recall = TP/(TP + FN)$$

The F1 score [13] is the harmonic average between accuracy and recall. The formula is as follows:

$$\text{F1} - \text{score} = (2 * \text{Precision} * \text{Recall})/(\text{Precision} + \text{Recall})$$

In this article, five types of machine learning were used to evaluate CTG data. The dataset is divided into a training set and a testing set. The ratio of the training set to the test set is 7:3. Each model has the same data sample and features. The parameters of each model are fitted to the training set, and then the performance of the model is verified on the test set. The results are shown in Fig. 4:

The results show that XGBoost, lightGBM, and Random trees belonging to set learning methods have shown exemplary performance in various indicators. Its accuracy is very high. Its generalization ability has good performance. The results indicate that these machine-learning methods can help doctors.

From the results (Table 3), it can be seen that XGBoost, lightGBM, and Random trees belonging to set learning methods have shown good performance in various indicators. Its accuracy is very high. Its generalization ability has good performance. The research paper concludes that XGBoost had the best performance among the evaluated models for assessing the fetus health status using CTG data. It suggests that machine learning methods can be feasible in evaluating the health status of the fetus and provide doctors with an objective assessment to assist in clinical diagnosis. The

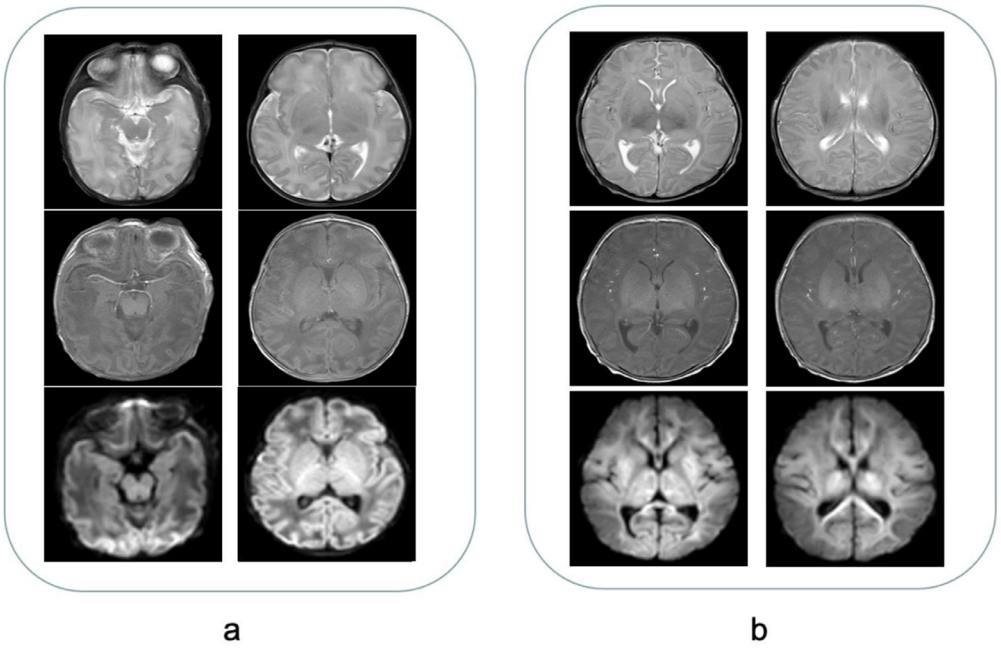

Fig. 3. Asphyxiated premature infants undergo magnetic resonance imaging within seven days after birth to observe the effect of asphyxia on the nervous system.

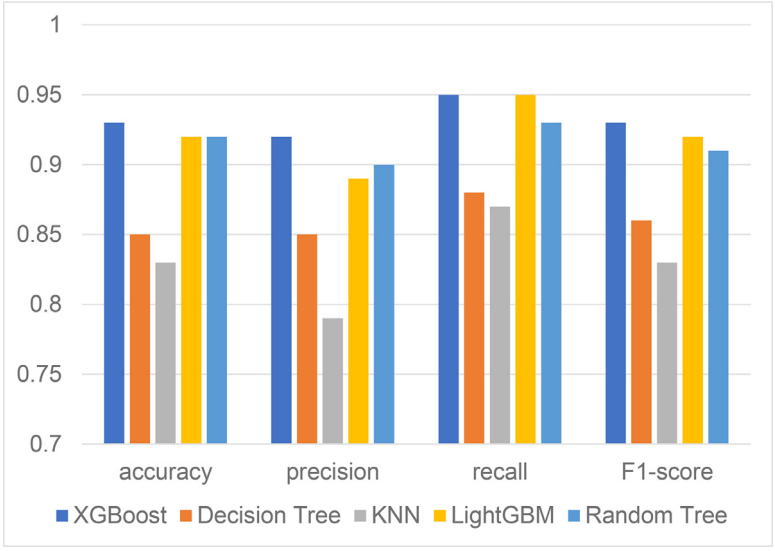

Fig. 4. shows that the accuracy of each model exceeds 80%, with XGBoost having the highest accuracy, reaching 93%. Other models include random trees (92%), lightGBM (92%), decision trees (85%), and KNN (83%). The performance of this model on other indicators is XGBoost (accuracy: 92%, recall rate: 95%, F1 score: 92%), random tree (accuracy: 90%, recall rate: 93%, F1 score: 91%), lightGBM (accuracy: 89%, recall rate: 95%, F1 score: 92%), decision tree (accuracy: 85%, recall rate: 88%, F1 score: 86%), KNN (accuracy: 79%, recall rate: 87%, F1 score: 83%).

text does not provide a direct comparison between machine learning models and traditional methods used by doctors in CTG analysis. However, the study suggests that machine learning methods can provide an objective assessment to assist doctors in clinical diagnosis, indicating a potential advantage over traditional methods.

Table 3
The performance of this model on other indicators.

	Accuracy	Precision	Recall	F1 score
XGBoost	92%	90%	93%	90%
Random tree	90%	88%	91%	89%
LightGBM	89%	87%	93%	90%
Decision tree	83%	83%	86%	84%
KNN	81%	77%	85%	81%

4. Discussion

The fetus hypoxia during pregnancy can cause serious consequences, as permanent brain injury, mental retardation, cerebral palsy, and even fetal death [14]. Electronic fetal monitoring (EFM) is considered as a very important method for fetal monitoring. The fetal heart monitoring has been proved to reduce the neonatal mortality [15]. The health status of the fetus can be reflected by the waveform of fetal heart rate (FHR) and uterine contraction (UC) obtained by EFM. However, because obstetricians evaluate the fetus's health status by analyzing the FHR and UC wave patterns displayed on the drawings, its accuracy must rely on obstetricians' experience and subjective judgment, which may lead to differences in the evaluation results of the same CTG. Moreover, even low-risk pregnant women are recommended to monitor 1 ~ 2 times

a week, which will increase the workload of clinicians and may lead to more errors in the evaluation results.

In order to standardize and guide obstetricians' evaluation criteria for CTG reports, the International Federation of Gynecology and Obstetrics (FIGO) [16], the National Institute of child health and human development (NICHD) [17], and the National Institute for Clinical Excellence (NICE) [18] have given corresponding fetal heart monitoring guidelines. These corresponding parameters: fetal heart rate baseline, fetal heart rate acceleration, fetal heart rate deceleration, and baseline variation, can be obtained by CTG. The fetal heart rate baseline refers to the fetal heart rate without fetal movement and uterine contraction. The normal FHR is 110–160 bpm (beat per minute). The acceleration of fetal heart rate is to form an upward convex wave peak at the baseline of fetal heart rate. The peak of fetal heart rate is $> =$ 15 bpm higher than the baseline of fetal heart rate, and the duration of the acceleration process is $> =$ 15 s. The average fetal heart rate is monitored at least thrice in 20 min. The deceleration of fetal heart rate is to form a downward concave peak at the baseline of fetal heart rate. The peak of fetal heart rate is $< =$ 15 bpm higher than the baseline of fetal heart rate, and the duration of the acceleration process is $< =$ 15 s. Abnormal fetal heart rate may indicate fetal intrauterine hypoxia and endanger fetal health. The fetus's health status can be monitored safely and timely through fetal heart rate monitoring.

With the development of computer technology, computer-aided diagnosis system has developed rapidly in hospitals and institutions. Obstetricians can easily read all parameters of FHR with the help of a diagnostic system. With the development of big data and the enhancement of computing power, the application of machine learning in medical treatment is also a research trend. There are also relevant studies running on fetal data. Spilka [19] selected 20 features in the data and trained the model by using SVM. G. Georgoula collected the time domain features, the frequency domain features and some morphological features from the fetal heart rate signal. They trained and compared the performance of SVM through the combination of different features to select the most appropriate features and classify the fetal condition [20]. Fergus used the recursive feature eliminator algorithm (RFE) and the features from FIGOand NICE to select and compare the performance of FLDA, RF, DL, and SVM [21–22]. This paper will use five machine-learning methods to classify fetal data. The experimental results show that the machine learning method can effectively assist obstetricians in diagnosis.

Neonatal asphyxia is an essential factor in perinatal infant mortality and disability, with a global incidence rate of 0.72–6.86% [25]. According to literature reports, multiple pregnancies, premature delivery, diabetes or hypertension during pregnancy, placental abruption, fetal distress, etc., are the main risk factors for neonatal asphyxia [26,27], among which premature delivery is the most common. After asphyxia and hypoxia in preterm infants, there will be an apparent secondary organ distribution and cerebral blood flow distribution. For example, the blood flow in the cerebral cortex is significantly reduced in the watershed area [28]. When hypoxia continues, the cardiovascular and cerebrovascular regulation function is disordered, and cerebral blood flow is insufficient, resulting in ischemic hypoxic brain injury [29,30], leading to neonatal disability or death. Due to the less complete development of the central nervous system in premature infants compared to full-term infants, the clinical manifestations of brain injury are not significant, and the pathological features of the nervous system are not easily identified, making the diagnosis of ischemic hypoxic encephalopathy more complex [31]. Early neonatal head MRI changes can provide pediatricians with information for diagnosis and treatment to indicate the prognosis and timely intervention on the nervous system's different effects to improve the newborn's quality of life in the future.

For future implementation, brain scan image segmentation based on advanced machine learning techniques [32] in the field of cybernetical intelligence [33] can enhance medical diagnosis and neurological investigation [34].

5. Conclusion

Fetal monitoring of pregnant women during the perinatal period is critical and is related to fetal health. Perinatal asphyxia is the leading cause of neonatal hypoxic-ischemic encephalopathy and one of the leading causes of neonatal death and disability. Severe asphyxia can cause brain damage and permanent nervous system damage, leaving different degrees of nervous system sequelae. The data displayed by CTG is an essential reference for evaluating fetal conditions. Doctors' evaluation of these data is subjective and cannot provide objective judgments. In this article, we used UCI's open-source CTG database, which contains a total of 2126 data, which is a three-classification problem. We divided the dataset into a training set: test set=7:3 and used five machine learning methods for training. They are XGBoost, lightGBM, random tree, KNN, and decision tree. The performance of XGBoost is the best among all models. It can accurately display the size and direction of blood flow velocity through vector arrows, accurately presenting the hemodynamic characteristics of cerebral blood vessels, and is the most valuable hemodynamic detection tool [23]. In addition, magnetic resonance imaging is non-invasive, easy to operate, and can continuously monitor changes in cerebral blood flow at the bedside, making its application very popular [24]. Early monitoring of cerebral blood flow in asphyxiated premature infants and early prediction and detection of brain injury have important guiding significance for clinical intervention and treatment. This will also provide objective assessments for pediatricians and obstetricians to assist in clinical diagnosis.

Ethics approval

All human subjects in this study have given their written consent for participation in our research.

Data availability

Data is available on request from the authors due to privacy/ethical restrictions.

Funding

This work was supported by Liaoning Provincial Department of Education Scientific Research Project (QNZR202012), Henan Pediatric Disease Clinical Medical Research Center Foundation (YJZX202207), CAAE Epilepsy Research Fund (CX-B -2021-02), Medical Education Research Project of Liaoning Province (2022-N004-09).

Declaration of Competing Interest

The authors declare no conflict of interest for this paper.

Acknowledgments

This research work received assistance from obstetricians and radiologists.

References

[1] Jie Qiao, Yuanyuan Wang, Xiaohong Li, et al., A lancet commission on 70 years of women's reproductive, maternal, newborn, child, and adolescent health in China, The Lancet (2021) Published online: May 24, 2021, doi:10.1016/S0140-6736(20)32708-2.

[2] P. Fergus, M. Selvaraj, C. Chalmers, Machine learning ensemble modeling to classify cesarean section and vaginal delivery types using Cardiotocography traces, Comput. Biol. Med. 93 (2018) 7–16.
[3] A. Subasi, B. Kadasa, E. Kremic, Classification of the cardiotocograph data for anticipation of fetal risks using bagging ensemble classifier, Procedia. Comput. Sci. 168 (2020) 34–39.
[4] D. Ayres-de-Campos, J. Bernardes, A. Garrido, et al., SisPorto 2.0: a program for automated analysis of cardiotocograms. J. Maternal Fetal Med. 9 (5) (2000) 311–318.
[5] Z.M.V. Kovács, R. Guerrieri, A generalization technique for nearest-neighbor classifiers, in: Proceedings of the IEEE International Joint Conference on Neural Networks. IEEE, 1991, pp. 2740–2745.
[6] J.R Quinlan, Induction of decision trees, Mach. Learn 1 (1986) 81–106.
[7] L. Breiman, Classification and Regression trees, Routledge, 2017.
[8] L.G Valiant, A theory of the learnable, Commun. ACM 27 (11) (1984) 1134–1142.
[9] R.E Schapire, The strength of weak learnability, Mach. Learn 5 (1990) 197–227.
[10] L. Breiman, Bagging predictors, Mach. Learn 24 (1996) 123–140.
[11] W.L. Qin, W.J. Zhang, C. Lu, Rolling bearing fault diagnosis based on ensemble empirical mode decomposition, information entropy, and random forests, Vibroeng. Procedia 5 (2015) 211–216.
[12] T. Chen, C. Guestrin, Xgboost: a scalable tree boosting system, in: Proceedings of the 22nd ACM signed international conference on knowledge discovery and data mining, 2016, pp. 785–794.
[13] Paul Fergus, Malarvizhi Selvaraj, Carl Chalmers, Machine learning ensemble modeling to classify cesarean section and vaginal delivery types using Cardiotocography traces, Comput. Biol. Med. 93 (2018) 7–16 ISSN 0010-4825, doi:10.1016/j.compbiomed.2017.12.002.
[14] G. Ke, Q. Meng, T. Finley, et al., Lightgbm: a highly efficient gradient boosting decision tree—Advances in neural information processing systems, 2017, 30.
[15] E. Chandraharan, S. Arulkumaran, Prevention of birth asphyxia: responding appropriately to cardiotocograph (CTG) traces, Best Pract. Res. Clin. Obstet. Gynaecol. 21 (4) (Aug. 2007) 609–624.
[16] Craig Barstow, Gauer, et al., How does electronic fetal heart rate monitoring affect labor and delivery outcomes? J. Family Pract. (2010).
[17] A. Ayres De Campos, FIGO consensus guidelines on intrapartum fetal monitoring: physiology of fetal oxygenation and the main goals of intrapartum fetal monitoring, Int. J. Gynecol. Obstet. 131 (1) (2015) 5–8.
[18] National Certification Corporation, NICHD Definitions and Classifications: application to Electronic Fetal Monitoring Interpretation, NCC Monograph. 3 (1) (2010) 1–20.
[19] V.S. Talaulikar, V. Lowe, S. Arulkumaran, Intrapartum fetal surveillance, Obstet.Gynaecol. Reprod. Med. 24 (2) (2014) 45–55.
[20] J. Spilka, J. Frecon, R. Leonarduzzi, N. Pustelnik, P. Abry, M. Doret, Sparse support vector machine for intrapartum fetal heart rate classification, IEEE J Biomed. Health Inform. 21 (3) (May 2017) 664–671, doi:10.1109/JBHI.2016.2546312.
[21] G. Georgoulas, D. Stylios, P. Groumpos, Predicting the risk of metabolic acidosis for newborns based on fetal heart rate signal classification using support vector machines, IEEE Trans. Biomed. Eng. 53 (5) (May 2006) 875–884, doi:10.1109/TBME.2006.872814.
[22] P. Fergus, A. Hussain, D. Al-Jumeily, et al., Cesarean section and regular vaginal deliveries are classified using fetal heart rate signals and advanced machine learning algorithms, BioMed. Eng. OnLine 16 (2017) 89, doi:10.1186/s12938-017-0378-z.
[23] L.L.L. Yeo, V.K. Sharma, Role of transcranial Doppler ultrasonography in cerebrovascular diseas, Recent Patents on CNS Drug Discov. (Discontinued) 5 (1) (2010) 1–13.
[24] D. Ratanakorn, Ultrasound Technique to Detect Internal Jugular Valve Incompetence and Clinical Implication, Ultrasound Med. Biol. 43 (2017) S216–S217.
[25] M. Obladen, From “apparent death” to “birth asphyxia”: a history of blame, Pediatr. Res. 83 (2) (2018) 403–411.
[26] J.P. Bouiller, M. Dreyfus, G. Mortamet, et al., Intrapartum asphyxia: risk factors and short-term consequences[J], J. Gynecol. Obstet. Biol. Reprod. (Paris) 45 (6) (2015) 626–632.
[27] F. Nayeri, M. Shariat, H. Dalili, et al., Perinatal risk factors for neonatal asphyxia in Vali-e-Asr hospital, Tehran-Iran, Iran J. Reprod. Med. 10 (2) (2012) 137.
[28] Z.A. Vesoulis, A.M Mathur, Cerebral autoregulation, brain injury, and the transitioning premature infant, Front. Pediatr. 5 (2017) 64.
[29] A.R Laptook, Birth asphyxia and hypoxic-ischemic brain injury in the preterm infan, Clin. Perinatol. 43 (3) (2016) 529–545.
[30] A. Nuñez, I. Benavente, D. Blanco, et al., Oxidative stress in perinatal asphyxia and hypoxic-ischaemic encephalopath, Anales de Pediatría (English Edition) 88 (4) (2018) 228 e1-228. e9.
[31] C.A. Herrera, R.M Silver, Perinatal asphyxia from the obstetric standpoint: diagnosis and interventions, Clin. Perinatol. 43 (3) (2016) 423–438.
[32] K.K.L. Wong, W. Xu, M. Ayoub, Y.L. Fu, H. Xu, R.Z. Shi, M. Zhang, F. Su, Z.G. Huang, W.M. Chen, Brain image segmentation of the corpus callosum by combining Bi-Directional Convolutional LSTM and U-Net using multi-slice CT and MRI, Comput. Methods. Programs. Biomed. 107602 (2023).
[33] K.K.L. Wong, M. Ayoub, Z. Cao, C. Chen, W. Chen, D.N. Ghista, C.W.J. Zhang, The synergy of cybernetical intelligence with medical image analysis for deep medicine: a methodological perspective, Comput. Methods. Programs. Biomed. (2023).
[34] L. Shi, W. Lou, A. Wong, F. Zhang, J. Abrigo, W.C.W. Chu, T.C.Y. Kwok, K.K.L. Wong, D. Abbott, D. Wang, V.C.T. Mok, Neural evidence for long-term marriage shaping the functional brain network organization between couples, Neuroimage 199 (2019) 87–92.